Dalton Transactions

Accepted Manuscript

ROYAL SOCIETY OF CHEMISTRY

www.rsc.org/dalton

Iron(III)-binding of the anticancer agents doxorubicin and vosaroxin

Katja Dralle Mjos,[a] Jacqueline F. Cawthray,[a] Gene Jamieson,[b] Judith A. Fox,[b] and Chris Orvig[a]*

[a]Medicinal Inorganic Chemistry Group, University of British Columbia, Department of Chemistry, 2036 Main Mall, Vancouver, British Columbia, V6T 1Z1, Canada

[b]Sunesis Pharmaceuticals, Inc., 395 Oyster Point Boulevard, South San Francisco, California, 94080, USA.

*Email: orvig@chem.ubc.ca

Abstract

The Fe(III)-binding constant of vosaroxin, an anticancer quinolone derivative, has been determined spectrophotometrically and compared with the analogous Fe(III) complex formed with doxorubicin. The *in vivo* metabolic stability and iron coordination properties of the quinolones compared to the anthracylines may provide significant benefit to cardiovascular safety. The mechanism of action of both molecules target the topoisomerase II enzyme. Both doxorubicin (Hdox, log β_{FeL3}= 33.41, pM= 17.0) and vosaroxin (Hvox, log β_{FeL3}= 33.80(3), pM= 15.9) bind iron(III) with comparable strength; at physiological pH however, [Fe(vox)$_3$] is the predominant species in contrast to a mixture of species observed for the Fe:dox system. Iron(III) nitrate and gallium(III) nitrate at a 1:3 ratio with vosaroxin formed stable tris(vosaroxino)-iron(III) and tris(vosaroxino)gallium(III) complexes that were isolated and characterized. Their redox behavior was studied by CV, and their stereochemistry was further explored in temperature dependent ^{1}H NMR studies. The molecular pharmacology of their interaction with iron(III) may be one possible differentiation in the safety profile of quinolones compared to anthracyclines in relation to cardiotoxicity.

Introduction

Anthracycline anticancer drugs, such as doxorubicin (Hdox) (Chart 1), are in broad use clinically but are associated with cumulative-dose cardiomyopathy.[1-6] Molecular mechanisms for doxorubicin induced cardiomyopathy remain controversial,[3,7] despite decades of investigations that have been recently reviewed.[5,8] These include interaction of doxorubicin with topoisomerase IIβ and induction of deoxyribonucleic acid (DNA) damage,[9,10] accumulation in normal myocardium,[11] metabolic conversion including the formation of damaging species,[12-17] and the generation of oxidative stress resulting from the interaction of doxorubicin with oxygen catalyzed by iron.[18,19] Through iron-mediated interactions, doxorubicin causes the formation of reactive oxygen species (ROS) such as hydrogen peroxide (H_2O_2) and superoxide radical anion ($O_2^{\cdot-}$). As depicted in Figure 1, the univalent reduction (e^-) of the aromatic core of the doxorubicin molecule gives the unstable semiquinone free-radical, doxoquinone, that in the presence of oxygen can auto-oxidize back to its parent quinone. The reduction of molecular oxygen leads to the formation of ROS which then can react further with free iron following the well-travelled pathways of Fenton chemistry, leading to an accumulation of iron in the mitochondria, increased levels of ROS, and overall impaired mitochondrial respiration.[8] The

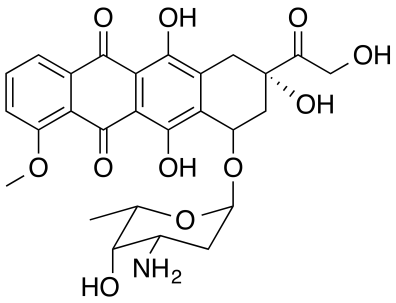

doxorubicin (Hdox)

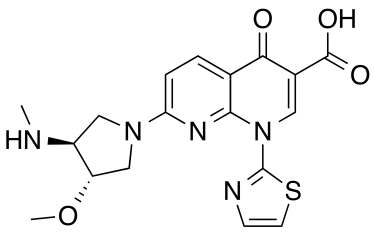

vosaroxin (Hvox)

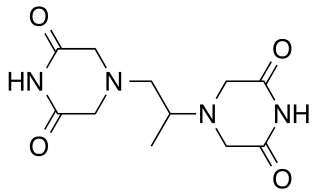

dexrazoxane

Chart 1 Chemical structures of doxorubicin (Hdox), vosaroxin (Hvox) and dexrazoxane.

bivalent reduction (2 e^-) of the side-chain carbonyl group of the doxorubicin molecule converts Hdox irreversibly into its secondary alcohol metabolite, doxol, which is slightly less redox active than the unstable semiquinone free-radical, therefore able to accumulate; doxol's disruptive effect on human Ca^{2+} and Fe^{3+} homeostasis appears stronger than the parent compound.[7] Reduction of Fe(III) to Fe(II) is an essential biological step that occurs widely in Nature.[20] On the molecular level, *in vivo* iron homeostasis is heavily regulated because living organisms carefully sequester iron(II) in stable complexes with biomolecules such as transferrin to prevent any toxicity arising from free iron overload. Reactive oxygen species, such as $O_2^{\cdot-}$, H_2O_2 as well as the hydroxyl radical ($OH^{\cdot}$), dramatically affect iron homeostasis in Nature. While ROS are involved in various essential biological functions, they can become harmful at higher concentrations, when their oxidation reaction of biomolecules increases physiological stress.[21] ROS species directly interact with ferrous and ferric ions *in vivo* in ways of Fenton oxidation chemistry.[22] Superoxide radical anions reduce Fe(III) that is coordinated to biological ligands to Fe(II) and dioxygen. In an inner-sphere electron-transfer mechanism, H_2O_2 oxidizes biologically-ligated Fe(II) to Fe(III) with concomitant formation of hydroxyl radical and hydroxide (HO^-) as reductive side-products, which leads to increased oxidative stress.

Oxidative stress is directly involved in the pathogenesis of heart failure; it damages the mitochondria through excess formation of $O_2^{\cdot-}$, reduction of adenosine triphosphate (ATP), and transcriptional alteration of genes associated with heart failure.[23,24] To circumvent induction of oxidative stress and cardiomyopathy, doxorubicin is administered with radical scavenger drugs, such as dexrazoxane (Chart 1), which reduce mitochondrial iron-levels.[25-27]

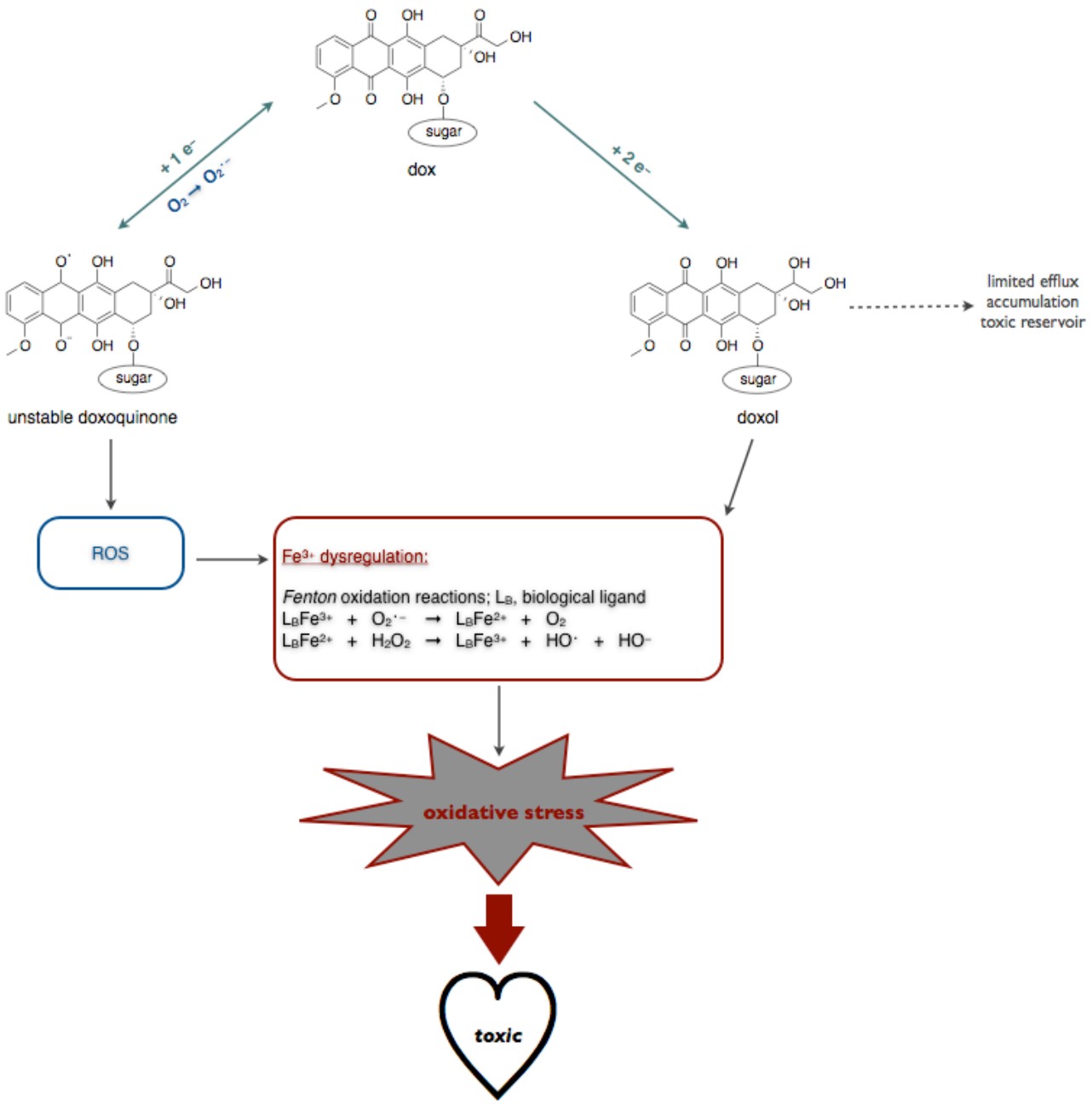

Fig. 1 Doxorubicin affects Fe^{3+} homeostasis *in vivo*: univalent reduction to semiquinone (left); bivalent reduction to secondary alcohol (right).

Vosaroxin (Hvox, Chart 1) is a first-in-class anticancer quinolone derivative (AQD) that induces DNA damage and inhibits topoisomerase II, inducing site-selective DNA damage, G2 arrest and apoptosis.[28-30] Vosaroxin induces DNA double/strand breaks (DSB) in cancer cells in G/C-rich sequences analogous to those caused by quinolone antimicrobials in bacteria.[28,31] In contrast to doxorubicin, vosaroxin is not a substrate for the multidrug resistance protein P-glycoprotein[32] and evades resistance mechanisms associated with p53 deficiencies.[33,34] Vosaroxin has been studied in both solid tumor cancers,[35,36] as well as hematologic malignancies,[37] and it is currently completing a phase 3 clinical trial in patients with relapsed or refractory acute myeloid leukemia.[38] In contrast to doxorubicin, vosaroxin's anticancer activity appears to result exclusively from intercalation of DNA and inhibition of topoisomerase II. Unlike doxorubicin, vosaroxin is minimally metabolized,[14,17,39] and thereby produces limited free radicals ROS via intrinsic metabolic activation.[28] As previously discussed, cardiomyopathy is a serious side-effect of treatment with doxorubicin, which has been associated with the formation of ROS and other toxic metabolites partly catalyzed by iron.

The fact that quinolones coordinate metals in various oxidation states in different coordination geometries[40] is a known side-effect for antimicrobial therapy, as such coordination leads to a reduction in quinolone bioavailability.[41] Iron(III) complexes with various commercially available quinolone antimicrobial drugs in which the iron coordinates the drug ligands in a stable octahedral 1:3 fashion have been reported and studied.[42-49] Iron(III) forms some of the most stable complexes with quinolones compared to other bivalent and trivalent metals,[50] and the determined stability constants range from log β_{FeL3} = 25.16 (0.005) for enoxacin[1] to log β_{FeL3} = 46.94 (8) for ciprofloxacin[2].

[1] HL= enoxacin, determined potentiometrically: 22°C, I(NaCl)= 0.1 M, inert gas N_2.[50]
[2] HL= ciprofloxacin, extrapolated from potentiometric data: 25°C, I(KCl)= 0.2 M.[51]

Antimicrobial treatment with quinolone drugs is, in general, considered safe, as they are known to be commonly well tolerated and have safety profiles that compare to those of other antimicrobial drug classes.[52-54] Frequently reported mild adverse reactions affect the gastrointestinal (GI) tract (e.g. nausea, vomiting, diarrhea) and the central nervous system (dizziness, headache, drowsiness), while tendinitis and tendon rupture as well as phototoxicity[55] are more severe side-effects for which certain quinolone antimicrobial agents are widely known.[29,30,52-54,56]

The molecular mechanisms of actions of vosaroxin, a quinolone derivative, and doxorubicin, an anthracycline, are differentiable as a result of their distinct chemical scaffolds (Chart 1). In order to further understand the properties of these two compounds, the interaction of vosaroxin with iron(III) has been characterized, and solution spectrophotometric studies of iron(III) coordination chemistry with vosaroxin and doxorubicin conducted. In addition, the novel tris(vosaroxino)iron(III) complex has been synthesized and characterized in order to examine the iron(III) coordination properties of vosaroxin in direct comparison to doxorubicin. Because the Ga^{3+} ion possesses many chemical similarities with the Fe^{3+} ion, their chemical binding properties are similar, especially in regard to ligand chelation or protein binding.[57] Biological systems cannot distinguish between Fe^{3+} and Ga^{3+}, a fact exploited in Fe^{3+} transport studies *in vivo*[58] or imaging[59]. Therefore, the diamagnetic tris(vosaroxino)gallium(III) analog has been synthesized as well, which allowed thorough NMR-studies of the isolated complex.

Experimental

Materials

Doxorubicin and iron(III) nitrate nonahydrate were purchased from Sigma-Aldrich, gallium(III) nitrate nonahydrate was obtained from Alfa-Aesar, and dimethyl sulfoxide (DMSO) was from Fisher Scientific. Sunesis Pharmaceuticals, Inc. provided the vosaroxin (reference standard quality, lot #12AK0025B). Deuterated dimethyl sulfoxide was purchased from Cambridge Isotope Laboratories, Inc., and Sigma-Aldrich delivered the deuterium oxide as well as the phosphoric acid-d_3 solution and the sodium deuteroxide. The atomic iron(III) standard solution for AAS (1000 mg L^{-1} ± 4 mg L^{-1}) was obtained from Fluka. In the preparation of all aqueous solutions for spectrophotometric measurements and syntheses, only deionized water, purified through a ELGA PURELAB ultrapure water system with a resistivity of 18 MΩ·cm (25 °C), was used.

Instrumentation

Melting points were determined using a Stanford Research Systems DigiMelt SRS melting point apparatus and are uncorrected. Ultraviolet-visible (UV-vis) spectrophotometry was performed on a Hewlett Packard 8453 instrument. Spectra were recorded using the UV-vis ChemStation Software (version B.04.01[61], Agilent Technologies, 2001−2010), and all maximum absorption bands and extinction coefficients (ε) are listed. Infrared (IR) spectra were recorded in the solid state on a PerkinElmer Frontier Fourier transformation (FT) IR spectrometer in the range 4000−650 cm^{-1} using the software PerkinElmer Spectrum (version 10.03.02, 2011). Only the most characteristic bands were interpreted using the following abbreviations: s, strong; m, moderate; w, weak; br, broad; sh, shoulder. Nuclear magnetic resonance (NMR) data (1D, 2D)

were collected on a BRUKER AV600 spectrometer (600 MHz). The residual solvent signal of the deuterated solvent was used as the internal standard.[60] Chemical shifts δ are referenced in ppm against tetramethylsilane (δ= 0). Multiplicities are abbreviated as: s, singlet; m, multiplet; br, broad. Ar represents aromatic protons. All spectra were analyzed with the software inmr (version 5.3.4, Mestrelab Research). Low-resolution mass spectral analysis was performed on a Water ZQ spectrometer equipped with electrospray and chemical ionization (ESCI) sources. High-resolution (HR) mass spectra were obtained at the UBC Mass Spectrometry (MS) Centre on a Waters Micromass LCT employing electrospray-ionization (ESI). Only characteristic signals have been listed as the dimensionless mass-to-charge ratio (*m/z*), with intensity related to the base signal.

Spectrophotometry

The instrumental set-up comprised a Corning Hot Plate Stirrer PC-351, a Fisher Scientific Accumet Basic pH-meter and a ThermoFischer ORION 8103BN ROSS Semi-Micro Combinational pH-electrode, which was calibrated before each titration using reference solutions (pH 4.00, 7.00, 10.00) from the FisherScientific Buffer-Pac. All solutions were prepared in aqueous sodium chloride (I = 0.15 M). Stock solutions of vosaroxin and doxorubicin were prepared as follows: about 1 mg of Hvox, or about 1.5 mg of Hdox, respectively, was dissolved in 5.00 mL sodium chloride solution, and after 30 min of sonication the suspension turned to a clear, colorless solution; these stock solutions were stable and used for 2-3 days. Solutions of ligand (Hvox, Hdox) only (~ 2.0×10^{-5} M) or ligand (Hvox, Hdox) (~ 2.0×10^{-5} M) mixed with iron(III) standard solutions in Fe^{3}:HL ratios of 1:1, 1:2 or 1:3 in a total volume of 10.00 mL were freshly prepared on the day of the experiment. To ensure that the titration started with the fully

protonated species of ligand, the ligand solutions were prepared in aqueous hydrochloric acid (0.2 M). The freshly prepared solution was sonicated for 15 min and transferred into a glass vial before the electrode was submerged in the test solution. The solution was stirred and the electrode remained submerged in the solution throughout the titration. The data were collected as pH vs. volume of titrant (2-20 μL). For each determination of ligand protonation constant or Fe(III) complexation constant, titrations were conducted in triplicate. Equilibration times between additions ranged from 3-10 min. All titration data were manipulated in MS Excel and plotted using Plot2 (version 2.0, Michael Wesemann). HypSpec (Protonic Software, Leeds) was used to fit the obtained UV-Vis curves to obtain the stability constants.

Computational Details

Calculations of vosaroxin with iron(III) were performed using Density Functional Theory (DFT) at the B3LYP level utilising the 6-31+g(d,p) basis set as implemented in Gaussian.[61] All optimised geometries are characterised as minima as indicated by the absence of imaginary frequencies. Geometry optimisations were performed on the systems and were evaluated to obtain stable Fe^{3+}:vosaroxin structures. Computational modelling was used to verify the binding site of the Fe^{3+} ion to Hvox. The initial geometry of vosaroxin was optimised and was used in a series of subsequent calculations whereby the Fe^{3+} ion was placed at various regions around the vosaroxin ligand but at distances greater than ~ 3.5 Å not to bias the interaction, if any, between the Fe^{3+} ion and the potential binding partner.

Synthesis and Characterization of Tris(vosaroxino)iron(III), [Fe(vox)$_3$]

Dissolving vosaroxin (125 mg, 0.31 mmol) in deionized water (20 mL) and stirring for 15 min at ambient temperature gave a clear, colorless solution of neutral pH. This solution was added dropwise into a previously prepared solution of iron(III) nitrate nonahydrate (40 mg, 0.1 mmol) in deionized water (5 mL). During the addition the pH was adjusted to < 3, if necessary, with aqueous hydrochloride solution (0.1 M). Upon completion of the addition, the pH was raised to pH 5 with aqueous sodium hydroxide (1.0 M), changing the color of the reaction mixture to red-brown. The reaction mixture was stirred at ambient temperature overnight, before the solvent was removed *in vacuo* to result an amorphous, lustrous, dark red-brown solid, which was washed repeatedly with deionized water and methanol, and then thoroughly dried *in vacuo* (108 mg, 0.086 mmol, 86%). **Mp** ≥ 200˚C, decomposition to black-brown solid. **UV-Vis** (DMSO): λ (ε) [$M^{-1}cm^{-1}$] = 275 (80000), 250 (50000). **IR**: $\tilde{\nu}$ [cm^{-1}] = 3433 (w, br), 3083 (w), 2997 (w), 2941 (w), 2881 (w), 2832 (w), 2732 (w), 2462 (w, br), 1621 (s), 1562 (sh), 1494 (s), 1443 (m), 1419 (m), 1317 (w), 1293 (w), 1276 (w), 1253 (s), 1178 (w), 1097 (s), 1038 (m), 968 (m), 921 (m), 854 (w), 825 (w), 803 (s), 758 (s), 722 (w), 701 (w), 675 (m). **MS** (ES+, methanol): m/z (%) = 1280 (< 10) [$ML_3 + Na^+$], 857 (100) $[ML_2]^+$. **HR-ESI-MS** m/z for $C_{54}H_{54}{}^{56}FeN_{15}O_{12}S_3{}^{39}K^+$ calcd. (found): 1295.2225 (1295.2233).

Synthesis and Characterization of Tris(vosaroxino)gallium(III), [Ga(vox)$_3$]

Vosaroxin (125 mg, 0.31 mmol) was dissolved in deionized water (12 mL) and stirred at ambient temperature for 10 min. The clear colorless vosaroxin solution was added drop-wise into a solution of gallium(III) nitrate nonahydrate in deionized water (5 mL). The reaction mixture turned pale yellow during the addition and its pH increased to pH 5. Without further adjustments,

the reaction solution was stirred at ambient temperature overnight. Removal of the solvent *in vacuo* gave an amorphous, lustrous, pale yellow solid that was washed repeatedly with water and methanol, and then thoroughly dried *in vacuo* (69 mg, 0.082 mmol, 82%). **Mp** ≥ 190 °C , decomposition to brown solid. **UV-Vis** (DMSO): λ (ε) [$M^{-1}cm^{-1}$] = 275 (80000), 250 (50000). **IR**: $\tilde{\nu}$ [cm^{-1}] = 3421 (m, br), 3086 (w), 3001 (w), 2937 (w), 2874 (w), 2832 (w), 2733 (w), 2473 (w, br), 1615 (s), 1564 (sh), 1494 (s), 1446 (m), 1423 (m), 1318 (w), 1277 (w), 1256 (s), 1179 (w), 1098 (s), 1040 (m), 970 (m), 923 (s), 858 (w), 826 (w), 803 (s), 760 (s), 728 (w), 702 (w), 680 (m). **NMR**: $\boldsymbol{\delta_H}$ (400 MHz, 363 K, d_6-DMSO) [ppm] = 10.05 (s), 9.96 (s), 9.79 (s), (3 H, $C_{ar_2}H$); 8.42 (d, $^3J_{HH}$ = 8.9 Hz), 8.33 (d, $^3J_{HH}$ = 9.1 Hz), 8.21 (d, $^3J_{HH}$ = 7.8 Hz), (3 H, $C_{ar_5}H$); 7.91-7.80 (m, 6 H, $C_{taz_4}H$ and $C_{ar_6}H$); 7.00 (d, $^3J_{HH}$ = 9.1 Hz), 6.90 (d, $^3J_{HH}$ = 7.2 Hz), (3 H, $C_{taz_5}H$); 4.30-4.26 (m, 3 H, $C_{azo_3}H$); 4.12-3.78 (m, 15 H, $C_{azo_5}H_2$, $C_{azo_4}H$, 3.43 $C_{azo_2}H_2$); 3.43 (s, 9 H, OCH_3); 2.68 (d, $^3J_{HH}$ = 17.4 Hz, 9 H, NH(CH_3)). $\boldsymbol{\delta_C}$ (150 MHz, 298 K, d_6-DMSO) [ppm] = 178.4, 176.1, 174.5 (C_{ar_4}); 165.0, 164.9, 164.8 (*C*OOH); 157.3, 157.1, 157.0 (C_{ar_7}); 155.6, 155.5, 155.4 (C_{taz_2}); 147.9, 147.7, 146.5 ($C_{ar_{8'}}$); 144.4, 144.1, 143.4 (C_{ar_2}); 138.4, 138.1, 137.9 (C_{taz_4}); 136.4, 136.2, 135.8 (C_{ar_5}); 122.3, 122.1, 121.8 (C_{ar_6}); 110.7, 110.6, 110.4 ($C_{ar_{4'}}$); 110.0, 109.8, 109.6 (C_{taz_5}); 109.9, 109.0, 108.8 (C_{ar_3}); 79.5, 79.4, 79.3 (C_{azo_3}); 60.7, 60.6, 60.5 (O*C*H$_3$); 57.2, 57.1, 57.0 (C_{azo_2}); 53.8, 53.7, 53.6 (C_{azo_5}); 50.7, 50.6, 50.5 (C_{azo_4}); 31.9, 31.8, 31.7 (N*C*H$_3$). **LR-MS** (ES+, CH_3OH): m/z (%) = 1272 (50) [$ML_3 + H^+$], 869 (100) $[ML_2]^+$. **HR-ESI-MS** m/z for $C_{54}H_{54}{}^{69}GaN_{15}O_{12}S_3{}^{23}Na^+$ calcd. (found): 1292.2392 (1292.2397); m/z for $C_{36}H_{36}{}^{69}GaN_{10}O_8S_2{}^+$ calcd. (found): 869.1415 (869.1414).

Electrochemistry

Cyclic voltammetry (CV) studies were performed with Hvox, [Fe(vox)$_3$] and [Ga(vox)$_3$] in a dimethyl sulfoxide solution (V = 10.0 mL) containing 0.1 M of tetra(*n*-butyl)ammonium perchlorate as the supporting electrolyte in a three electrode system composed of a platinum-disk electrode as the working electrode, a platinum-mesh electrode as the counter electrode and a silver electrode as the pseudo reference electrode. A potentiostat (Pine AFCBP1, ID 23051890) was integrated into the electric circuit. The software AfterMath.Inc. (version 1.2.4532) was used for controlling the potentiostat and recording the data. CV measurements followed standard procedures. All glassware was dried in the oven at 100 °C for 24 hours before use. Tetra(*n*-butyl)ammonium perchlorate (0.342 g, 0.001 mol) was transferred into the electrochemical cell and dried *in vacuo* for 15 min. In parallel, dimethyl sulfoxide was degassed with N_2 gas. Using Schlenk techniques, 10.0 mL of the degassed dimethyl sulfoxide was transferred onto the tetra(*n*-butyl)ammonium perchlorate inside the electrochemical cell. The mixture was stirred vigorously until the electrolyte salt had completely dissolved. Throughout the experiment the electrochemical cell was kept under N_2 gas at all times. Firstly, a blank voltammogram of the electrolyte solution was recorded. Secondly, the compound to be measured was added as a solid and dissolved in the electrolyte solution (0.01 mmol, respectively: Hvox**,** 41 mg; [Fe(vox)$_3$], 12.6 mg; [Ga(vox)$_3$] 12.0 mg). Measurements on these compounds were performed in the general voltage range between + 1.3 V and - 2.3 V, starting from an initial voltage of 0 V and ending at a final voltage of 0 V. The sweep rate was 100 mV·s^{-1}, the electrode range was varied between 5−10 μA, and the number of segments was set to 5 as default. The experiment concluded with a reference measurement of ferrocene. All electrodes were cleaned accordingly. The platinum-mesh electrode and the silver pseudo-reference electrode were submerged in methanol (separate

vials) and sonicated for 30 min. The platinum-disk electrode was polished using Buehler MicroPolish II Alumina Powder (0.3 μm and 0.05 μm); polish residues were rinsed off with deionized water and the electrode was dried.

Results and Discussion

Stability Constants

Vosaroxin and doxorubicin each contain ionizable protons. The pK_a values for each ligand, as determined by spectrophotometric titration, are given in Table 1. In acidic solutions, doxorubicin exists as the singly charged species $[H_2dox]^+$ with the positive charge at the sugar amino group. Initial dissociation (pK_a 7.67) is assigned to the amino sugar group followed by the dissociation of the phenolic hydrogens (pK_a 9.46 and 10.96). These assignments are in agreement with those in the literature.[62] It is interesting to note that there is some variation in literature data on the amino group pK_a value 6.8–8.99,[63] and pK_a of 9.01–11.2 for the phenolic group. These differences can be attributed, in part, to self-association and decomposition of the drug at higher concentrations (> 30 μM).[64] The concentrations of doxorubicin used in the present studies were purposefully low enough to avoid self-association (~20 μM). Vosaroxin has four ionizable protons, existing as the triply charged species $[H_4vox]^{3+}$ under acidic conditions. The pK_a values determined in this study are in close agreement with those extrapolated from a co-solvent system.[65] The small differences observed may be attributed to the use of sodium chloride at biologically relevant concentrations (I = 0.15 M) as background electrolyte in our studies. We are in agreement with the ionization process previously established.[65]

The formation of the Fe(III)-doxorubicin and Fe(III)-vosaroxin complexes as a function of pH and $[Fe^{3+}]$:[HL] molar ratios was investigated by spectrophotometric titration. The formation of the Fe^{3+}-doxorubicin complexes elicited broad absorption bands centered at 600 nm (see the Electronic Supporting Information, ESI), as previously reported.[63,66,67] Experiments with Fe(III)-doxorubicin proved problematic due to drifting electrode measurements, formation and precipitation of $Fe(OH)_3$ as well as low concentrations of complex formed under the experimental conditions utilized. Despite the apparent distance between the amino group and the iron binding site of doxorubicin, the charge on the amino group is known to influence the strength of interaction with the metal ion.[68] These problems interfered with convergence within HypSpec when fitting the data, and there were large uncertainties in the log *K* values that were obtained. Consequently, the log *K* values for doxorubicin presented in Table 1, have been taken from the literature.[62]

The visible absorption spectra of solutions containing Fe(III) and vosaroxin as a function of pH (ESI) are characterized by a new, broad absorption band centered around 400 nm as shown in Figures 2 and 3. In order to fit the iron(III)-vosaroxin titration data, it was necessary to select a model incorporating all possible species. We have utilized computational modelling in order to identify the preferred binding site of the Fe^{3+} ion to vosaroxin.[69] For this, we performed geometry optimisation (energy minimization) calculations on different states whereby the Fe^{3+} ion was placed at various locations around the vosaroxin ligand; however, not to bias the interaction, the Fe^{3+} ion was never placed in a distance closer than ~ 3.5 Å to vosaroxin, the potential binding partner. The most stable conformer involves the ferric ion being chelated by the ketone oxygen and the deprotonated carboxylate moiety (Figure 4). It is interesting to note that energy minimisation of vosaroxin alone or in the presence of iron results in rotation of the

thiazole ring such that the orientation of this group differs between bound and unbound species. For unbound vosaroxin, the thiazole group is almost co-planar with the naphthyridine ring and the sulfur atom nearest the ring nitrogen atoms. Following complexation of Fe^{3+} at the diketone, the thiazole group rotates so it is now almost at a right angle to the naphthyridine ring. This was confirmed by scanning the potential energy surface for rotation around the N-C bond of the thiazole, and is consistent with the ^{1}H NMR data collected following titration of Fe^{3+} with vosaroxin. These data show that addition of Fe^{3+} influences the chemical shift of neighboring hydrogens including those around the thiazole and naphtyridine rings, not just those expected to be influenced by chelation (data presented in ESI).

Table 1 Protonation and Fe^{3+} formation constants for doxorubicin and vosaroxin.

	Doxorubicin	**Vosaroxin**
log K_{110}	17.985*	16.31(3)
log K_{120}	11.049	8.70(2)
log K_{130}	4.379	7.80(3)
log β_{130}	33.413	32.80(3)
pM	17.0	15.9
pK_{a1}	10.96(1)	9.97(2)
pK_{a2}	9.46(1)	7.091(4)
pK_{a3}	7.67(2)	5.125(4)
pK_{a4}		2.779(4)

pM = -log[Fe], pH 7.4, $[L]_T$ = 10 µM, $[Fe]_T$ = 1 µM. * 37 °C, I = 0.15 M (NaCl).[62]

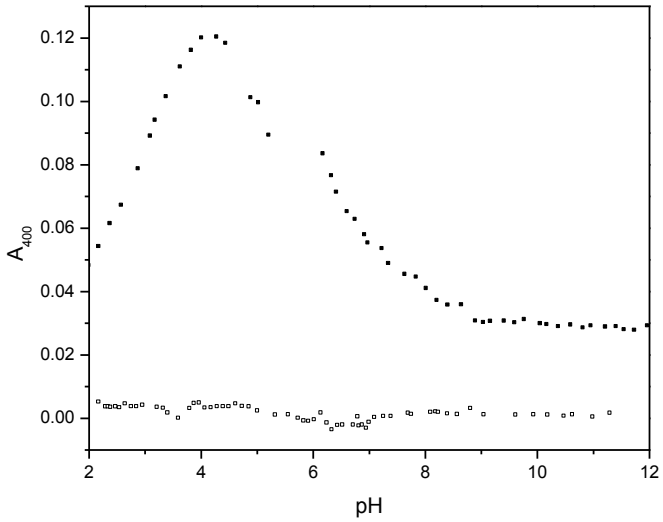

Fig. 2 Comparison of the changes in absorbance at 400 nm for a solution of Fe(III)-vosaroxin ($[Fe^{3+}] = 5.8 \times 10^{-6}$ and [vosaroxin] = 2.24×10^{-5} M) (■) and vosaroxin only (□) with varying pH in aqueous solution ($I = 0.15$, NaCl).

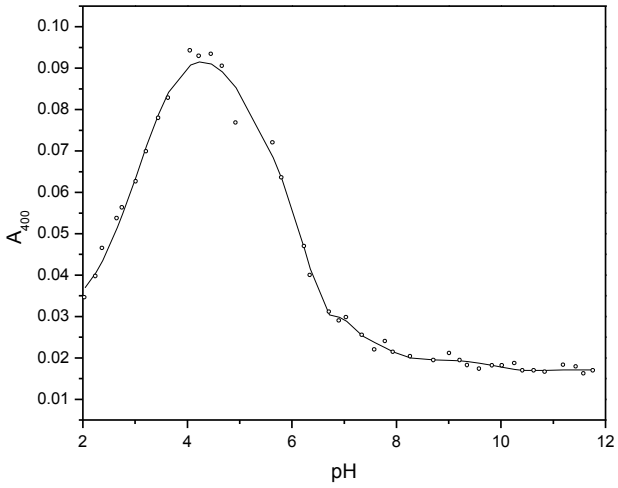

Fig. 3 Representative fit at 400 nm using obtained stability constants for a solution of Fe(III)-vosaroxin in 1:3 molar ratio: ○ experimental data, – fitted absorbance.

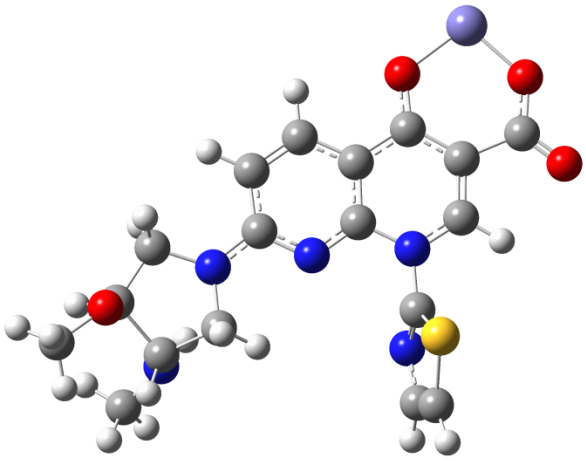

Fig. 4 Interaction of the Fe^{3+} ion (lavender) with one anion of vosaroxin, showing the most stable diketone-coordinated conformation obtained following energy minimization using B3LYP/6-31+g(d,p). The tris complex would have three such ligands around the Fe^{3+}.

Speciation plots for solutions of vosaroxin with Fe(III) as a function of pH are shown in Figure 5 (respective doxorubicin plot in ESI). At a ratio of 3:1 ligand to metal, the predominant species in the Fe(III)-doxorubicin system at pH 7.4 is the non-coordinated, singly charged ligand (H_3dox^+), in contrast to the Fe(III)-vosaroxin system where $[Fe(vox)_3]$ is the predominant species. This reflects the differences in both stability of the metal-ligand and metal-protonated ligand complexes, and also the ionization state of the ligands at physiological pH. For vosaroxin, the $[Fe(vox)_3]$ complex is the single, dominant species from pH 6.5 onwards into the basic pH range; however, the interaction between Fe^{3+} and doxorubicin appears to be more complex as

various species of iron coordinated and protonated doxorubicin are observed in the distribution. $[Fe(vox)_3]$ only slowly starts to form at pH 8 and higher, while at physiological pH free ligand

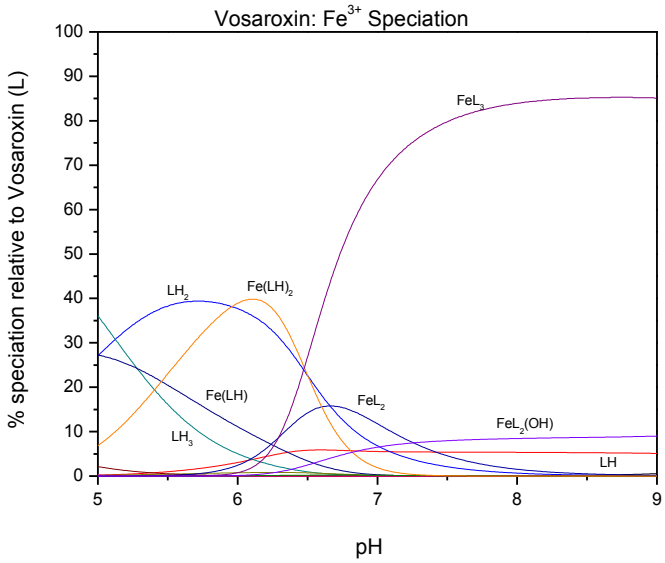

Fig. 5 Species distribution curves for the iron(III)-vosaroxin system. $[Fe^{3+}]_T = 3.3 \times 10^{-4}$ M, $[L]_T = 1 \times 10^{-3}$ M.

in various protonation states (H_2dox, H_3dox$^+$) exist next to the hydroxide adduct [Fe(dox)(OH)] . The latter is a minor species (≤ 30 %) between pH 6.5 – 9. In their study of the stability and iron coordination in DNA adducts of anthracycline based anticancer drugs, Ericksson and coworkers[70] found that the Fe^{3+} in the [dox-DNA]Fe^{3+} system was coordinated to four O-atoms belonging to the [dox-DNA] adduct, and was in addition coordinating five water molecules as well. They suggested that the lower number of O-atoms and the higher number of H_2O molecules bound to the Fe^{3+} were related to a lower binding energy of the metal ion possibly resulting in an increased production of hydroxyl radicals *in vivo*. This suggests that the $[Fe(vox)_3]$ species is potentially more thermodynamically stable, because the central Fe^{3+} is

coordinated to a total of six O-atoms of the three vox-ligands, versus the [Fe(dox)(OH)] species, in which the metal is only coordinated to two ligand O atoms and a hydroxide. The coordination number of iron(III) is six. In the $[Fe(vox)_3]$ complex, all six iron coordination positions are occupied leaving no access for further hydroxyl coordination to the unoccupied iron orbitals.

Synthesis and characterization tris(vosaroxino)iron(III) and -gallium(III) complexes

Aqueous solutions of vosaroxin were mixed with aqueous solutions of iron(III) nitrate nonahydrate, and gallium(III) nitrate nonahydrate respectively, in a 3:1 ratio (Scheme 1).

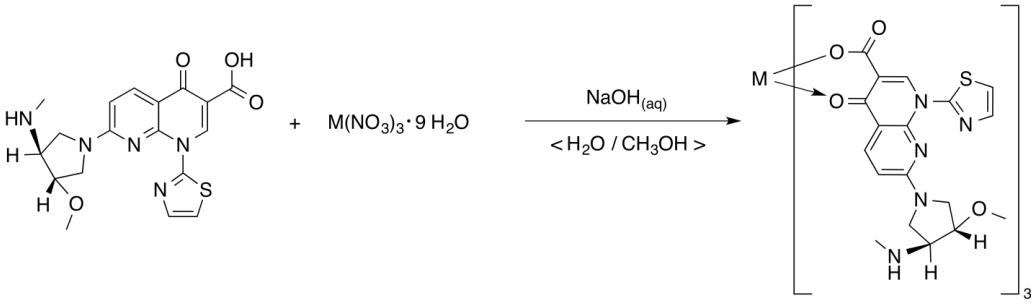

Scheme 1 Synthetic route to tris(vosaroxino)metal(III) complexes $[M(vox)_3]$, M = Fe^{3+}, Ga^{3+}.

The coordination of vosaroxin was favored over the formation of metal-hydroxide. species around pH 5, as indicated by the lack of precipitation due to hydroxide formation, and by MS-samples taken out of the reaction solution with a peak for ML_2^+ (100 %). Allowing the reaction solution to stand at ambient temperature, or in the fridge at 4 °C, for several days did not promote precipitation, and the MS signal continued to show that characteristic ML_2^+ peak (100 %). Upon removal of the solvent *in vacuo*, and thorough washing of the obtained solid with small amounts of water and methanol, the respective metal-vosaroxin complexes were isolated and characterized by high resolution electrospray ionization (HR-ESI) mass spectrometry. The

data were consistent with the formation of tris(vosaroxino)metal(III). The compounds are nonvolatile and stable, decomposing at approximately 200 °C. The solubility of the obtained $[M(vox)_3]$ (M= Fe^{3+}, Ga^{3+}) complexes is generally low and shows a high pH dependence; therefore, solution characterization of these complexes by MS was carried out with solutions in methanol, acetonitrile and nitromethane. Structure analysis by ^{1}H and ^{13}C NMR spectroscopy was only possible in d_6-DMSO due to the extremely low solubility of both complexes in D_2O and other standard NMR-solvents. This low solubility, in addition to the various stereoisomers, negatively impacted both elemental analyses and attempts to grow single crystals suitable for X-ray analysis of either complex. It has been reported previously that it is challenging to grow single-crystals of quinolone-metal complexes.[71] Over the past eighteen months, a multitude of attempts were undertaken to grow single crystals according to various crystallization methods and personal tricks of fellow researchers in the department. Diffusion methods in varying volumes, concentration and glass ware set-ups were used, employing mainly acetonitrile, chloroform, diethyl ether, DMSO, methanol and water, according to solubility. Respective crystallization vials were placed in the freezer, the fridge, on the window sill and in a dark cupboard at room temperature, but crystals suitable for single x-ray diffraction did not grow. In addition, reactive crystallization experiments were conducted, in which the starting materials were dissolved in different solvents over a range of pH conditions and layered on top of each other in one vial according to the density of the solvent. Unfortunately, the diffusion reaction did not lead to crystals but instead to an amorphous powder in some cases (systems of DMSO, methanol, water) or to no reaction at all.

The mass spectra, however, were diagnostic of the complex formulations at a 3:1 ratio of vosaroxin:metal. With both metal ions (Fe^{3+}, Ga^{3+}), loss of one ligand from a ML_3 unit was

observed giving the ML_2^+ fragment with 100 % intensity. In addition, the tris(vosaroxino)iron(III) complex in methanol cationized in the high-resolution ES+ by attachment of one sodium or potassium cation to form $[NaML_3]^+$ or $[KML_3]^+$ as the parent peak. $[Ga(vox)_3]$ was dissolved in low concentrations in various solvents (methanol, acetonitrile, nitromethane, DMSO) for further characterization with low- and high-resolution ES+ techniques. The spectra clearly reflected the effect of the different solvents on the mass pattern. In addition to the $[NaML_3]^+$ parent peak, recombination signals corresponding to $[M_2L_5]^+$ were observed for $[Ga(vox)_3]$ in nitromethane, which we have previously reported as characteristic for tris(ligand)metal(III) complexes.[72]

Spectroscopic analysis in the mid-infrared region (IR) (4000 − 650 cm^{-1}) supported the complete coordination of the respective metal through the carboxylate O atom. Although the IR spectra of the quinolones are in general quite complex because of the numerous functional groups in the molecule, the stretching frequencies of the carbonyl and carboxyl group are strong and can be identified as prominent absorption bands among the many and varied C_{aryl}–H and C–N vibrations in the same IR region.[40,71] The IR spectrum of the free ligand showed a strong characteristic band at 1728 cm^{-1} attributed to the stretching frequency of the carboxyl-OH-group on the aromatic ring system; upon coordination of Fe^{3+} or Ga^{3+} it disappeared completely, as the IR-spectra of the respective metal-vosaroxin complexes show (Figure 6). In the IR spectra of both vosaroxin-metal complexes, two distinct bands in the range 1620 − 1315 cm^{-1} could be assigned to the ν_{CO_2} asymmetric and symmetric stretching vibrations. The difference Δ [cm^{-1}]= $\nu_{asym}(CO_2)$ - $\nu_{sym}(CO_2)$ is quite large with Δ= 304 cm^{-1} for $[Fe(vox)_3]$, and Δ= 297 cm^{-1} for $[Ga(vox)_3]$, likely characteristic for a monodentate coordination mode of the carboxyl group.[73,74]

^{1}H NMR spectra of vosaroxin were recorded in D_2O as well as in d_6-DMSO, showing a negligible solvent effect. Vosaroxin can form four different stereoisomers around the metal(III) center upon coordination of three bidentate anions in an octahedral fashion (possible stereoisomers of $[M^{3+}(vox)_3]$: Δ–*fac*; Λ–*fac*; Δ–*mer*; Λ–*mer*). In the case of the diamagnetic $[Ga(vox)_3]$, the different stereoisomers gave a multitude of signals in a ^{1}H NMR spectrum recorded at 298 K, but at 393 K the interchange happened so rapidly on the NMR time scale that a separation of signals occurred and a clear assignment was possible (T dependent NMR study

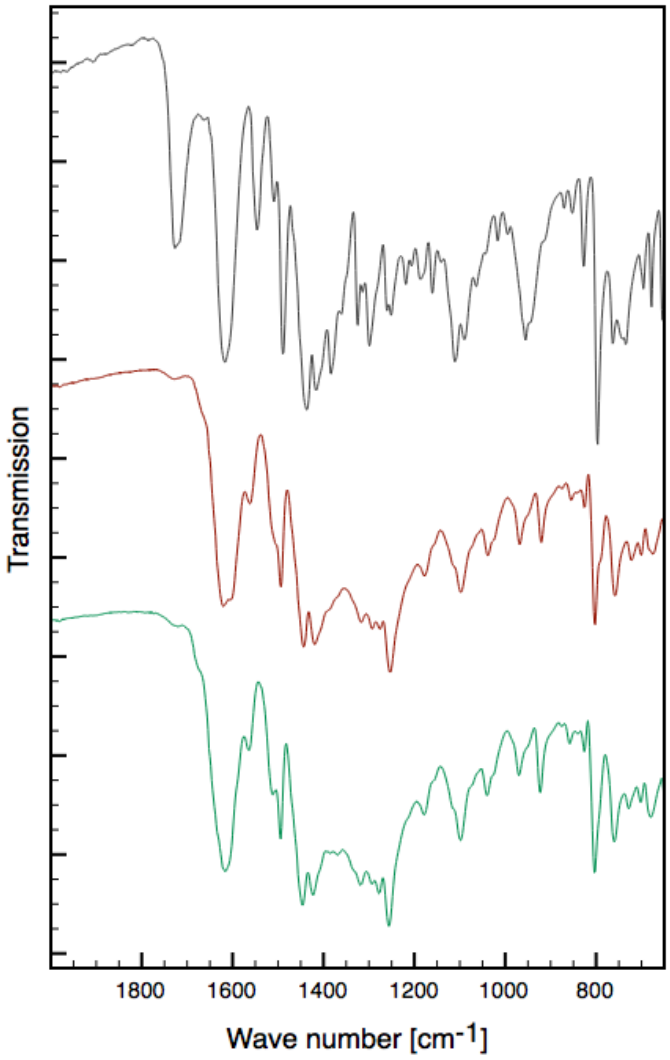

Fig. 6 IR spectra of vosaroxin (Hvox, black, top), [Fe(vox)$_3$] (red, middle) and [Ga(vox)$_3$] (green, bottom); the spectrum of Hvox shows the peak at 1728 cm^{-1} disappearing upon coordination to Fe^{3+} or Ga^{3+}.

presented in ESI). In the case of [Fe(vox)$_3$], the Fe^{3+} ion retains a paramagnetic high-spin state upon complexation. As a result, the NMR signals are broadened considerably and impossible to assign with certainty. In an attempt to support the DFT calculations, which favored coordination through the carboxyl-substituent and the carbonyl-group on the aromatic ring system, and to rule out experimentally that the metal was not also coordinated to vosaroxin via the nitrogen atoms at the substituent on $N_{ar}1$ and $C_{ar}6$, complexes were characterized by ^{1}H NMR after incremental addition of AAS-standard iron(III) solution. Vosaroxin (c= 5×10^{-4} M, V= 5 mL) was dissolved in deuterated phosphate buffer pH 7.20 (pD 7.0), as the ligand was insoluble in deuterated phosphate buffer at pH 2.15. Small increments (V= 2 µL) of AAS-standard iron(III) solution were added to the titration solution, which was then stirred rigorously for three minutes, before a sample of the solution (V= 0.5 mL) was transferred into an NMR tube. The titration was monitored via ^{1}H NMR at 600 MHz (data presented in ESI). Unfortunately, upon addition of iron(III) all NMR signals broadened significantly; therefore, it was impossible to detect a measurable increased broadening in the aromatic region, which would have supported coordination through the carboxyl-group on *C*-3 and the carbonyl-group on *C*-4, over the aliphatic region. This would indicate coordination via the substituent ring systems on $N_{ar}1$ and $C_{ar}6$. The experiment was further complicated by the precipitation of a dark red solid, (presumably [Fe(vox)$_3$]) from the solution, although the chemical identity of the precipitate could not be determined to our full satisfaction.

Cyclic voltammetry studies

To evaluate redox/decomplexation of $[Fe(vox)_3]$ and $[Ga(vox)_3]$, the complexes were studied via cyclic voltammetry (CV curves of Hvox and $[Ga(vox)_3]$ presented in ESI). For $[Fe(vox)_3]$ (Figure 7), the Fe(III)/Fe(II) couple at 0.771 V vs NHE[75] could not be clearly identified in the recorded cyclic voltammogram. The cyclic voltammogram, while irreversible, was found to be reproducible over multiple cycles without a large decrease of intensities of either peak. For the Fe(III) as well as for the Ga(III) complex of vosaroxin, a dissimilar peak shape was observed, which indicates a reorganization in the coordination sphere and therewith the coordination symmetry around the metal center upon reduction of the metal, as had been previously observed for tris(ciprofloxacino)iron(III).[45]

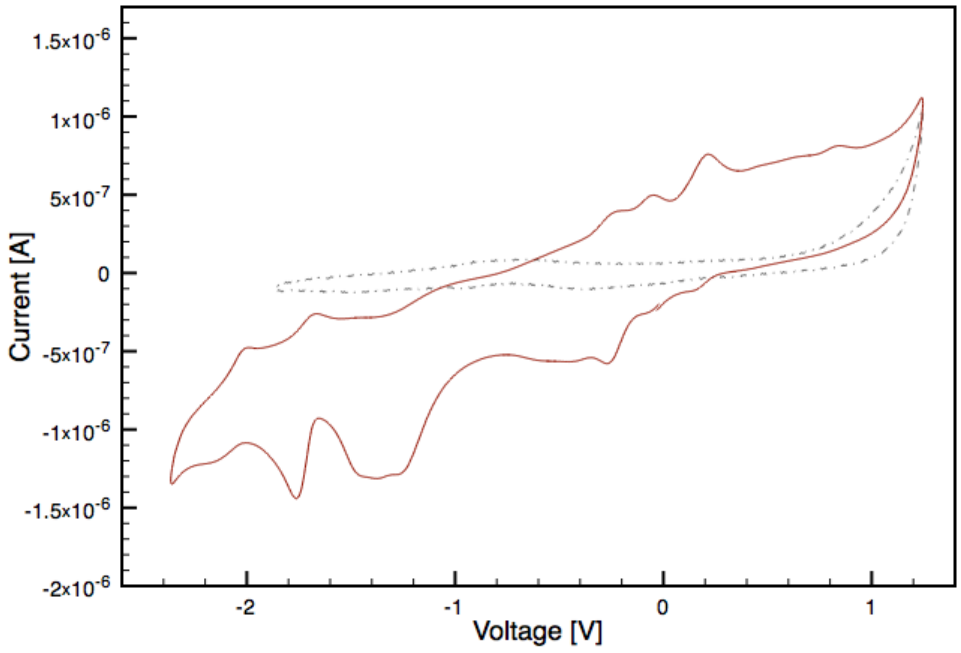

Fig. 7 Cyclic voltammograms, 0.001 M $[Fe(vox)_3]$ in DMSO (red), 0.1 M tetra(*n*-butyl)ammonium perchlorate, scan rate 100 $mV \cdot s^{-1}$ (background, grey).

Conclusions

Spectrophotometric titrations in 0.15 M NaCl, at ambient temperature, in the pH range from pH 2 – 12, showed that the two anticancer agents doxorubicin and vosaroxin bind Fe^{3+} with similar strength; however, at physiological pH, $[Fe(vox)_3]$ is the predominant species in contrast to the mixture of protonated ligand species observed for the Fe:doxorubicin system. Here, H_2dox (~30%) and H_3dox^+ (~40%) in addition to the minor (~30%) [Fe(dox)(OH)] are observed, indicating a more labile interaction between Fe^{3+} and doxorubicin than between Fe^{3+} and vosaroxin at physiological pH. Furthermore, two novel vosaroxin-metal(III) complexes were successfully synthesized. In tris(vosaroxino)iron(III) as well as in tris(vosaroxino)gallium(III), the metal ion is coordinated through the deprotonated carboxylate oxygen on the naphthyridine ring system in a monodentate coordination mode leading to the formation of four stereoisomers. The diamagnetic $[Ga(vox)_3]$ complex was studied by NMR at different temperatures. For the $[Fe(vox)_3]$ complex, the iron redox couple was observed in the recorded CV spectrum. We report the characterization of stable complexes of vosaroxin, an anticancer quinolone derivative, with gallium(III) and iron(III). These results are consistent with the well-studied clinical and chemical interaction between iron preparations (ferrous gluconate/sulfate, various multivitamin preparations) and quinolone-based drug molecules.[76] When co-administered, the ferrous iron is oxidized to its ferric form, which rapidly forms quite stable tris(quinolono)iron(III) complexes. *In vivo*, the quinolones are very likely stable in the presence of iron[77] in contrast to the anthracyclines whose interaction with iron presumably leads to the formation of free radicals and lipoperoxidation.[18,19] The stable $[Fe(vox)_3]$, dominant at physiological pH, is unlikely to produce toxic metabolites and ROS associated with the more labile interaction from doxorubicin and

Fe^{3+}. The data presented here suggest that vosaroxin treatment may not result in the cumulative-dose cardiotoxicity associated with doxorubicin.

Acknowledgements

The authors acknowledge Dr. Maria Ezhova and Dr. Zhicheng (Paul) Xia for help with the NMR measurements; Dr. Yun Ling for assistance with the MS measurements of [Ga(vox)$_3$]; and Caterina Ramogida and Jeff Therien for support with the CV measurements. The authors thank the University-Industry Liaison Office (UILO) of the University of British Columbia for facilitating this fruitful collaboration, and NSERC Canada for on-going Discovery Grant support.

Notes

Electronic Supplementary Information (ESI) available: UV-vis spectra of one titration run of vosaroxin to determine the pK_as of the test solution, of Hvox:Fe in the ratio of 1:1, of Hvox:Fe in the ratio of 2:1, of Hvox:Fe in the ratio of 3:1; as well as UV-vis spectra of one titration run of doxorubicin to determine the pK_as of the test solution, of Hdox:Fe in the ratio of 1:1, of Hdox:Fe in the ratio of 2:1, of Hdox:Fe in the ratio of 3:1; cyclic voltammetric curves for 0.001 M of vosaroxin (Hvox) and [Ga(vox)$_3$] in DMSO solution containing tetra(*n*-butyl)ammonium perchlorate 0.1 M at a scan rate of 100 $mV \cdot s^{-1}$; ^1H NMR spectra of the titration of Hvox with Fe^{3+} at pD 7 (deuterated phosphate buffer) at 298 K; ^1H NMR spectra of the temperature dependence study conducted on [Ga(vox)$_3$] in the range of 298 – 363 K, species distribution curves for the iron(III)-doxorubicin system, characterization of vosaroxin.

Abbreviations

ATP	Adenosine triphosphate
AQD	Anticancer quinolone derivative
CV	Cyclic voltammetry
DFT	Density functional theory
DMSO	Dimethyl sulfoxide
DNA	Deoxyribonucleic acid
DSB	Double/strand breaks in DNA
ESCI	Electrospray and chemical ionization
FT	Fourier transformation
GI	Gastrointestinal tract
Hdox	Doxorubicin
HR-ESI	High-resolution electrospray ionization
Hvox	Vosaroxin
IR	Infrared
NMR	Nuclear magnetic resonance
MS	mass spectrometry
m/z	mass-to-charge ratio
ROS	Reactive oxygen species
UV-vis	Ultraviolet-visible

References

1 M.S. Ewer: *Chapter 2 - Anthracycline Cardiotoxicity: Clinical Aspects, Recognition, Monitoring, Treatment and Prevention*. In M.S. Ewer and E.T.H. Yeh (Eds.): *Cancer and the Heart*, People's Medical Publishing House, Shelton CT, 2nd edn., 2013.

2 P.K. Singal and N.I. Iliskovic, *N. Engl. J. Med.,* 1998, **339**, 900-905.

3 D.A. Gewirtz, *Biochem. Pharmacol.*, 1999, **57**, 727-741.

4 G. Minotti, P. Menna, E. Salvatorelli, G. Cairo and L. Gianni, *Pharmacol. Rev*., 2004, **56**, 185-229.

5 Y. Shi, M. Moon, B. McManus and P.P. Liu, *Herz*, 2011, **36**, 296-305

6 K. Chatterjee, J. Zhang, N. Honbo and J.S. Karliner, *Cardiology*, 2010, **115**, 155-162.

7 P. Menna, E. Salvatorelli and G. Minotti, *Chem. Res. Toxicol.*, 2008, **21**, 978-989.

8 F.S. Carvalho, A. Burgeiro, R. Garcia, A.J. Moreno, R.A. Carvalho and P.J. Oliveira, *Med. Res. Rev.*, 2014, **34**, 106-135.

9 Y.L. Lyu, J.E. Kerrigan, C.P. Lin, A.M. Azarova, Y.C. Tsai, Y. Ban and L.F. Liu, *Cancer Res*., 2007, **67**, 8839-8846.

10 S. Zhang, X. Liu, T. Bawa-Khalfe, L.S. Lu, Y.L. Lyu, L.F. Liu and E.T.H. Yeh, *Nat. Med*., 2012, **18**, 1639-1642.

11 R.S. Jaenke, D. Deprez-DeCampeneere and A. Trouet, *Cancer Res*., 1980, **40**, 3530-3536.

12 J.H. Doroshow, *Cancer Res*., 1983, **43**, 4543-4551.

13 J.H. Doroshow and K.J.A. Davies, *J. Biol. Chem.*, 1986, **261**, 3068-3074.

14 A. Bartoszek and C.R. Wolf, *Biochem. Pharmacol*., 1992, **43**, 1449-1457.

15 R.D. Olson, P.S Mushlin, D.E. Brenner, S. Fleischer, B.J. Cusack, B.K. Chang and R.J. Boucek Jr., *Proc. Natl. Acad. Sci. USA*, 1988, **85**, 3585-3589.

16 A. Cartioni, P. Menna, E. Salvatorelli, D. Braghiroli, R. Giampietro, F. Animati, A. Urbani, P. Del Boccio and G. Minotti, *J. Biol. Chem.*, 2004, **279**, 5088-5099.

17 B.N. Zordoky, M.E. Aboutabl and A.O. El-Kadi, *Drug Metab. Dispos.*, 2008, ***36***, 2277-2286.

18 X. Xu, H.L. Persson and D.R. Richardson, *Mol. Pharmacol.*, 2005, **68**, 261-271.

19 E. Gammella, F. Maccarinelli, P. Buratti, S. Recalcati and G. Cairo, *Front. Pharmacol.*, 2014, **5**, DOI:10.3389/fphar.2014.00025.

20 A.L. Feig and S.J. Lippard, *Chem. Rev.*, 1994, **94**, 759-805.

21 J. Prousek, *Pure Appl. Chem.*, 2007, **79**, 2325-2338.

22 H.J.H. Fenton, *J. Chem. Soc.*, 1894, **65**, 899-910.

23 K.B. Wallace, *Pharmacol. Toxicol.*, 2003, **93**, 105-115

24 H. Nojiri, T. Shimizu, M. Funakoshi, O. Yamaguchi, H. Zhou, S. Kawakami, Y. Ohta, M. Sami, T. Tachibana, H. Ishikawa, H. Kurosawa, R.C. Kahn, K. Otsu and T. Shirasawa, *J. Biol. Chem.*, 2006, **281**, 33789-33801.

25 Y. Ichikawa, M. Ghanefar, M. Bayewa, R. Wu, A. Khechaduri, A.V.Naga Prasad, R.K. Mutharasan, T.J. Naik and H. Ardehali, *J. Clin. Invest.*, 2014, **124**, 617-630.

26 G. Takemura and H. Fujiwara, *Progr. Cardiovasc. Dis*., 2007, **49**, 330-352.

27 B.B. Hasinoff, P.E. Schroeder and D. Patel, *Mol. Pharmacol.*, 2003, **64**, 670-678.

28 R.E. Hawtin, D.E. Stockett, J.A. Byl, R.S. McDowell, T. Nguyen, M.R. Arkin, A. Conroy, W. Yang, N. Osheroff and J.A. Fox, *PLoS ONE*, 2010, **5**, e10186, DOI:10.1371/journal.pone.0010186.

29 V.T. Andriole (Ed.): *The Quinolones*, Academic Press, San Diego, USA, 3rd edn., 2000.

30 D. C. Hooper and E. Rubinstein, Eds. *Quinolone Antimicrobial Agents*, ASM Press, Herndon, USA, 3rd edn., 2003

31 S.N. Richter, G. Giaretta, V. Comuzzi, E. Leo, L.A. Mitchenall, L.M. Fisher, A. Maxwell and M. Palumbo, *Nucleic Acids Res.*, 2007, **35**, 6075-6085.

32 U. Hoch, J. Lynch, Y. Sato, S. Kashimoto, F. Kajikawa, Y. Furutani and J.A. Silverman, *Cancer Chemother. Pharmacol.*, 2009, **64**, 53-65.

33 J. Hyde, J. Wright, N. Osheroff, J.A. Silverman, D.H. Walker and M.R. Arkin, *AACR Annual Meeting Abstracts*, 2005, 2293.

34 E.J. Walsby, S.J. Coles, S. Knapper and A.K. Burnett, *Haematologica*, 2011, **96**, 393-399.

35 R.H. Advani, H.I. Hurwitz, M.S. Gordon, S.W. Ebbinghaus, D.S. Mendelson, H.A. Wakelee, U. Hoch, J.A. Silverman, N.A. Havrilla, C.J. Berman, J.A. Fox, R.S. Allen and D.C. Adelman, *Clin. Cancer Res.*, 2010, **16**, 2167-2175.

36 L.M. Krug, J. Crawford, D.S. Ettinger, G.I. Shapiro, D. Spigel, T. Reiman, J.S. Temel, G.C. Michelson, D.Y. Young, U. Hoch and D.C. Adelman, *J. Thorac. Oncol.*, 2011, **6**, 384-386.

37 J.E. Lancet, F. Ravandi, R.M. Ricklis, L.D. Cripe, H.M. Kantarjian, F.J. Giles, A.F. List, T. Chen, R.S. Allen, J.A. Fox, G.C. Michelson and J.E. Karp, *Leukemia*, 2011, **12**, 1808-1814.

38 *Study of Vosaroxin or Placebo in Combination With Catarabine in Patients With First Relapsed or Refractory Acute Myeloid Leukemia (AML) (VALOR),* U.S. ClinicalTrials.gov Identifier: NCT01191801.

39 M.J. Evanchik, D. Allen, J.C. Yoburn, J.A. Silverman and U. Hoch, *Drug. Metab. Dispos*., 2009, **37**, 594-601.

40 V. Uivarosi, *Molecules*, 2013, **18**, 11153-11197.

41 R.E. Polk, *Am. J. Med.*, 1989, **87** (suppl. 5A), S76-81.

42 N. Barba-Behrens, G. Mendoza-Diaz and D.M.L. Goodgame, *Inorg. Chim. Acta*, 1986, **125**, 21-26.

43 S.A. Saadek, *J. Mol. Struct.*, 2005, **753**, 1-12.

44 E.K. Efthimiadou, A. Karaliota and G. Psomas, *Polyhedron*, 2008, **27**, 1729-1738.

45 G. Psomas, *J. Inorg. Biochem.*, 2008, **102**, 1798-1811.

46 N. Sultana, A. Naz, M.S. Arayne and M. Ahmed Mesaik, *J. Mol. Struct.*, 2010, **969**, 17-24.

47 E.K. Efthimiadou, A. Karaliota and G. Psomas, *J. Inorg. Biochem.*, 2010, **104**, 455-466.

48 H.F. Abd El-Halim, G.G. Mohamed, M.M.I. El-Dessouky and W.H. Mahmoud, *Spectrochim. Acta A*, 2011, **82**, 8-19.

49 S.C. Wallis, L.R. Gahan, B.G. Charles and T.W. Hambley, *Polyhedron*, 1995, **14**, 2835-2840.

50 B. Urbaniak and Z.J. Kokot, *Anal. Chim. Acta*, 2009, **647**, 54-59.

51 I. Turel, N. Bukovec and E. Farkas, *Polyhedron*, 1996, **15**, 269-275.

52 R. Stahlmann, H. Lode, *Drugs*, 1999, **Suppl.2**, 37-42.

53 C.M. Oliphant and G.M. Green, *Am. Fam. Physician*, 2002, **65**, 455-464.

54 R.C. Owens and P.G. Ambrose, *Clin. Infect. Dis.*, 2005, **41** (suppl. 2), S144-157.

55 H. Baes, *Dermatologica*, 1968, **136**, 61-64.

56 K. Marutani, M. Matsumoto, Y. Otabe, M. Nagamuta, K. Tanaka, A. Miyoshi, T. Hasegawa, H. Nagano, S. Matsubara, R. Kamide, T. Yokota, F. Matsumoto and Y. Ueda *Antimicrob. Agents Chemother.*, 1993, **37**, 2217-2223.

57 L.R. Bernstein, *Pharmacol. Rev.*, 1998, **50**, 665-682.

58 K.D. Weaver, J.J. Heymann, A. Mehta, P.L. Roulhac, D.S. Anderson, A.J. Nowalk, P. Adhikari, T.A. Mietzner, M.C. Fitzgerald and A.L. Crumbliss, *J. Biol. Inorg. Chem.,* 2008, **13**, 887-898.

59 G. Bandoli, A. Dolmella, F. Tisato, M. Porchia and F. Refosco, *Coord. Chem. Rev.*, 2009, **253**, 56-77.

60 H.E. Gottlieb, V. Kotlyar and A. Nudelman, *J. Org. Chem.*, 1997, **62**, 7512-7515.

61 *Gaussian 09*, Revision D.01, M.J. Frisch, G.W. Trucks, H.B. Schlegel, G.E. Scuseria, M.A. Robb, J.R. Cheeseman, G. Scalmani, V. Barone, B. Mennucci, G.A. Petersson, H. Nakatsuji, M. Caricato, X. Li, H.P. Hratchian, A.F. Izmaylov, J. Bloino, G. Zheng, J.L. Sonnenberg, M. Hada, M. Ehara, K. Toyota, R. Fukuda, J. Hasegawa, M. Ishida, T. Nakajima, Y. Honda, O. Kitao, H. Nakai, T. Vreven, J.A. Montgomery Jr., J.E. Peralta, F. Ogliaro, M. Bearpark, J.J. Heyd, E. Brothers, K.N. Kudin, V.N. Staroverov, R. Kobayashi, J. Normand, K. Raghavachari, A. Rendell, J.C. Burant, S.S. Iyengar, J. Tomasi, M. Cossi, N. Rega, N.J. Millam, M. Klene, J.E. Knox, J. B. Cross, V. Bakken, C. Adamo, J. Jaramillo, R. Gomperts, R.E. Stratmann, O. Yazyev, A.J. Austin, R. Cammi, C. Pomelli, J.W. Ochterski, R.L. Martin, K. Morokuma, V.G. Zakrzewski, G.A. Voth, P. Salvador, J.J. Dannenberg, S. Dapprich, A.D. Daniels, Ö. Farkas, J.B. Foresman, J.V. Ortiz, J. Cioslowski and D.J. Fox, Gaussian, Inc., Wallingford CT, USA, 2009.

62 P.M. May, G.K. Williams and D.R. Williams, *Eur. J. Cancer*, 1980, **16**, 1275-1276.

63 H. Beraldo, A. Garnier-Suillerot, L. Tosi and F. Lavelle, *Biochemistry*, 1985, **24**, 284-289.

64 F. Capolongo, M. Giomini, A.M. Giuliani, B.F. Matzanke, U. Russo, A. Silvestri, A.X. Trautwein, and R. Barbieri, *J. Inorg. Biochem.*, 1997, **65**, 115-122.

65 Quintiles, *SNS-595: pKa Analysis*, Technical report Q8802, 2005, Quintiles−Kansas City, USA.

66 M.M.L. Fiallo, H.T.B. Haj and A. Garnier-Suillerot, *Met. Based Drugs*, 1994, **1**, 183-193.

67 M.M.L. Fiallo, A. Garnier-Suillerot, B. Matzanke and H. Kozlowski, *J. Inorg, Biochem.*, 1999, **75**, 105-115.

68 D. Gelvan and A. Samuni, *Cancer Res*., 1988, **48**, 5645-5649.

69 K. Nawara, J.L. McCracken, P. Krysinski and G.J. Blanchard, *J. Phys. Chem. B.*, 2013, **117**, 6859-6867.

70 A. Eizaguirre, M. Yanez and L.A. Eriksson, *Phys. Chem. Chem. Phys.*, 2012, **14**, 12505-12514.

71 I. Turel, *Coord. Chem. Rev.*, 2002, **232**, 27-47.

72 M.M. Finnegan, T.G. Lutz, W.O. Nelson, A. Smith and C. Orvig, *Inorg. Chem.*, 1987, **26**, 2171-2176.

73 G.B. Deacon and R.J. Phillips, *Coord. Chem. Rev*., 1980, **33**, 227-250.

74 *Infrared and Raman Spectra of Inorganic and Coordination Compounds, Part B: Applications in Coordination, Organometallic, and Bioinorganic Chemistry*, K. Nakamoto, John Wiley & Sons, Inc., New York, USA, 5th edn., 1997.

75 *CRC Handbook of Chemistry and Physics*, ed. W.M. Haynes, Internet Version, 94th edn., 2014.

76 E.A. Hartshorn, B.M. Lomaestro and G.R. Bailie, *Ann. Pharmacother.*, 1991, **25**, 1249-1258.

77 M. Kara, B.B. Hasinoff, D.W. McKay, N.R.C. Campbell, *Br. J. Clin. Pharmacol.*, 1991, **31**, 257-261.

TOC

The two anticancer agents, doxorubicin and vosaroxin, bind Fe^{3+} with comparable strength; however, at physiological pH tris(vosaroxacino)iron(III) is the dominant species.

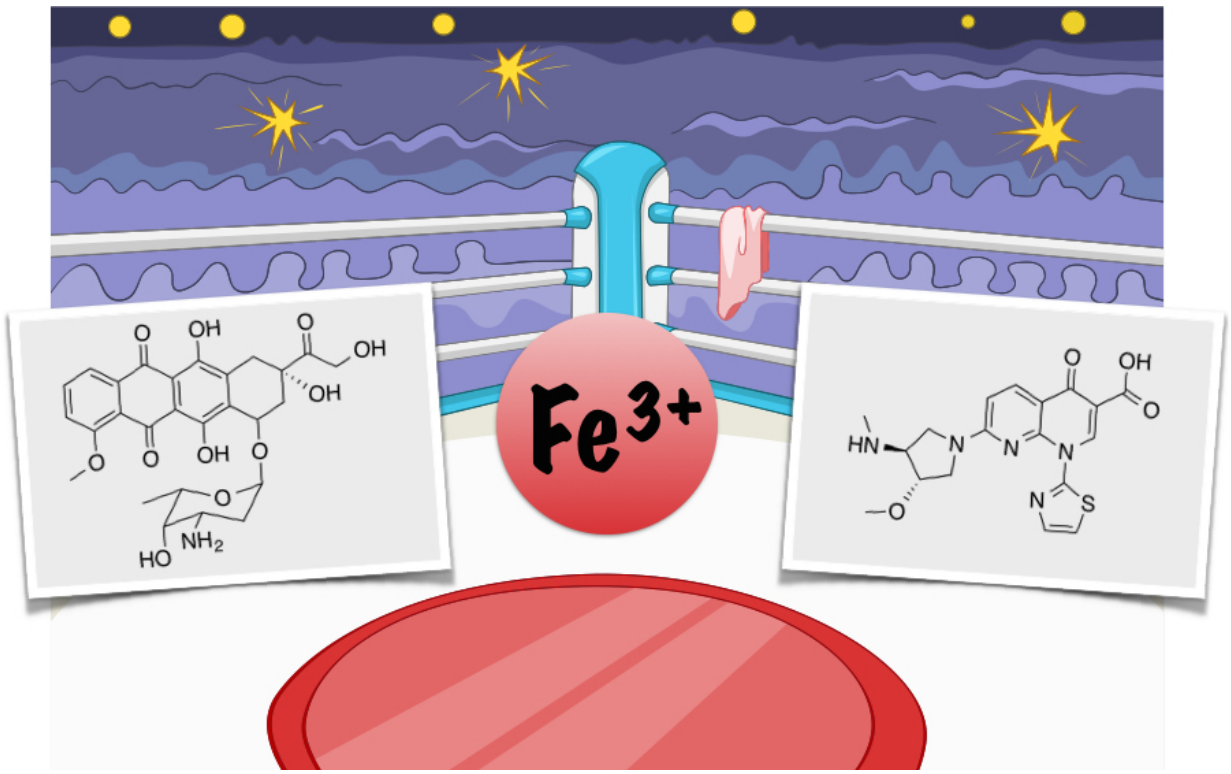

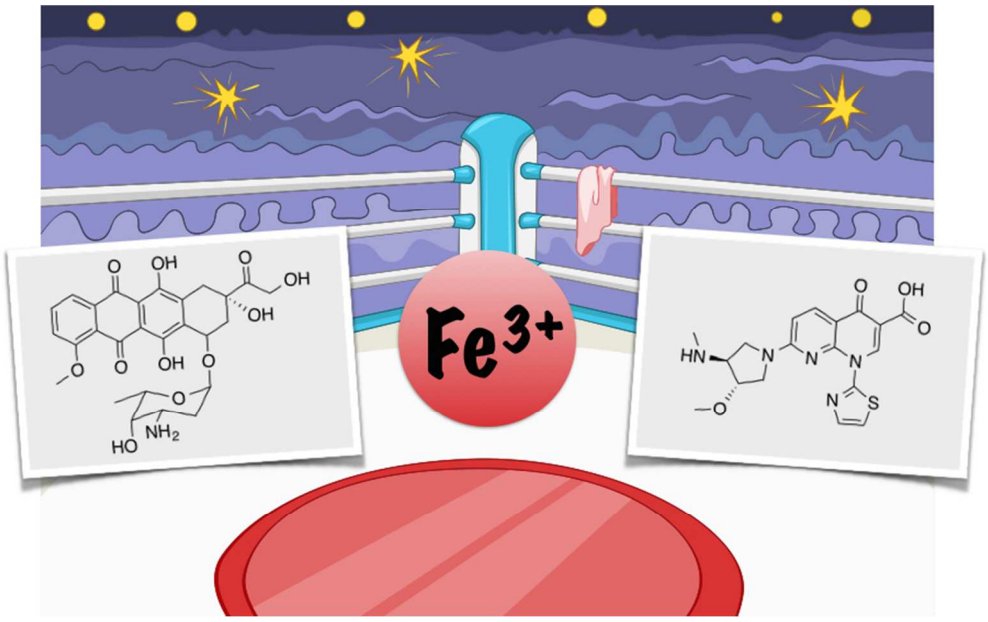

322x196mm (72 x 72 DPI)